coatings

Article

Enhancing the Efficiency of Ice-Resistant Materials in Asphalt Road Surfaces: A Comprehensive Performance Analysis

Xijuan Zhao [1], Yemao Zhang [2,*] and Mulian Zheng [3]

[1] Institute of Industrial Economy and Innovation Management, Nanjing Institute of Technology, Nanjing 211167, China; njdjzxj@126.com
[2] School of Civil Engineering and Architecture, Nanjing Institute of Technology, Nanjing 211167, China
[3] Department of Highway and Railway Engineering, School of Highway, Chang'an University, Xi'an 710064, China; zhengml@chd.edu.cn
* Correspondence: zhangyemao158@163.com

Abstract: This study addresses the critical issue of traffic safety in winter, particularly focusing on the challenges posed by ice and snow on roads. Traditional methods of snow and ice removal are often labor-intensive, inefficient, and environmentally harmful. The objective is to develop a more effective solution for asphalt pavement deicing. Inspired by the anti-icing coating technology used in high-voltage conductors, this research develops an ice-suppressing material designed to reduce the adhesion between snow, ice, and pavement surfaces. The material's performance is evaluated in terms of deicing efficiency, durability, adhesive properties, and its impact on pavement performance. Test results demonstrate that the developed ice-suppressing material significantly reduces the adhesion between the ice layer and the pavement, facilitating easier removal. This study concludes that the developed ice-suppressing material significantly enhances deicing efficiency on asphalt pavements. It exhibits strong hydrophobic properties, as evidenced by increased water droplet contact angles on coated surfaces (99.5° to 83.3°) compared to clean glass slides (39.2° to 29°). This hydrophobicity effectively reduces ice adhesion, decreasing tensile and shear strength of the ice layer by 38.2% and 63.6%, respectively. Additionally, the material demonstrates superior ice-melting capabilities in sub-zero temperatures, with coated ice cubes showing a higher mass reduction rate than uncoated ones. Importantly, its slow-release nature ensures sustained deicing performance over multiple cycles, maintaining effectiveness after seven test cycles. This study introduces an innovative ice-suppressing material that not only improves the efficiency and environmental impact of deicing methods but also contributes to enhancing road safety in winter conditions. The material's novel composition and sustained effectiveness present a significant advancement in the field of winter road maintenance.

Keywords: ice-suppressing materials; mix design; deicing performance; durable performance

check for updates

Citation: Zhao, X.; Zhang, Y.; Zheng, M. Enhancing the Efficiency of Ice-Resistant Materials in Asphalt Road Surfaces: A Comprehensive Performance Analysis. *Coatings* **2024**, *14*, 37. https://doi.org/10.3390/coatings14010037

Academic Editor: Valeria Vignali

Received: 22 November 2023
Revised: 22 December 2023
Accepted: 22 December 2023
Published: 27 December 2023

1. Introduction

Snow and ice on road pavements are common in most regions of China during winter. These conditions significantly reduce the road surface's adhesion coefficient and skid resistance, leading to decreased vehicle speed, extended travel times, increased fuel consumption, and even traffic accidents [1]. Furthermore, traffic issues caused by icy road conditions are a global concern [2]. Consequently, snow and ice melting have become integral components of winter road maintenance, carrying substantial economic and societal benefits [3]. Consequently, many nations prioritize the treatment of road snow and ice and have conducted extensive research. The literature has explored various solutions, including manual and mechanical removal, snow melting agent application, heated pavement systems, conductive concrete, freezing inhibition pavement technology, and ice-suppressing and coating technologies [4,5].

Ice-suppressing materials, which can lower the freezing point through embedded melting agents or isolate the ice layer from the road surface using hydrophobic materials, have emerged as effective solutions. These materials are applied to asphalt pavements through manual brushing or mechanical spraying [6]. When rain or snow falls, the ice-melting- and snow-removing materials on the carrier are released to melt snow and ice. Simultaneously, hydrophobic materials within the ice-suppressing material isolate the ice layer from the pavement, effectively reducing adhesion and facilitating easy removal. Compared to traditional deicing methods, ice-suppressing and coating technologies offer several advantages, including active ice and snow melting, excellent environmental performance, efficient and long-lasting deicing, and preventive capabilities [7].

Hydrophobic ice-suppressing technology originally found its application in the treatment of icing on high-voltage transmission lines [1]. This involved the application of a superhydrophobic nano-deicing coating material on the conductors, effectively reducing ice formation on the transmission lines. In the field of road science and technology, efforts have been made to develop anti-icing and thin-ice removal coatings using hydrophobic deicing technology for high-voltage transmission lines [8].

Ma et al. conducted a study on the anti-icing performance of asphalt pavement using hydrophobic surface and thin-ice removal pavement coating technology. They developed a coating technology with hydrophobic properties, inspired by the deicing mechanism employed for high-voltage conductors [9,10]. This technology involves the creation of a hydrophobic film on the asphalt pavement surface, which isolates the ice layer. However, this approach does not rely on self-melting capabilities. While some preliminary test sections were conducted, there is a lack of comprehensive documentation of the construction process, technology, and specialized construction machinery and equipment.

The concept of an environmentally friendly asphalt pavement snow and ice-melting coating technology was initially proposed by Yang [11]. This eco-friendly technology offers hydrophobic properties that reduce adhesion between the ice layer and the pavement. It also provides slow-release snow melting and deicing capabilities. Although the coating's performance has been studied, there is a lack of construction technical indicators, requirements, and specific construction tools and machinery tailored to the coating's features [12].

Several scholars have examined ice-suppressing materials and explored construction technologies based on the principles of ice and snow melting and ice suppression [4,13]. An anti-freeze ice-suppressing material for asphalt pavement was developed by adding a suitable amount of slow-release anti-icing agent (Mafilon) to emulsified asphalt. Tests were conducted to evaluate deicing effectiveness and conductivity at various Mafilon contents, including an experiment to determine the optimal spraying thickness of the ice-suppressing material. Siegmund Werner et al. used porous adsorption materials to absorb self-melting snow additives, achieving long-term snow melting through slow-release mechanisms [14]. Kaemereit Wilhelm et al. successfully prepared 0.5~1 mm granular self-melting snow additive material by utilizing cement as a carrier material through cement solidification [15]. The V-260 snow melting agent developed by Verglimit Company in Switzerland consists of calcium chloride-coated hydrophobic material and is widely used today [16].

In Japanese self-snow melting technology, porous zeolite is used as an absorbent to adsorb salt, which is then added to asphalt mixtures in powder form to replace fine aggregate or mineral powder. This approach achieves snow melting and ice removal through salt release [17–19]. China first introduced imported self-snow melting technology and materials around 2000. In recent years, many domestic road researchers have embarked on the study of self-snow melting technology [20]. Zhou et al. adopted Japanese snow melting technology to research and develop self-snow melting additives [21].

Ma et al. have researched and developed the granular snow melting admixture Iceguard, known for its slow-release- and non-corrosive properties. It is considered safe and environmentally friendly for the metal components of bridges and road structures [5]. Shan et al. conducted studies measuring pavement wettability after applying a hydrophobic coating, changes in stone absorption rates, and the length and density of cracks in the ice layer following the impact of a steel ball [22]. Zheng et al. conducted an analysis and evaluation of the deicing coating's performance from various perspectives, including anti-ice and snow performance, durability of the coating materials, and impact on pavement skid resistance [23]. Wu et al. developed a regression model for long-term snow melting performance and provided a calculation formula for determining the precipitation amount of additives on self-melting asphalt pavement in different regions of the country [24]. The long-term snow melting performance of asphalt mixtures with Iceguard was evaluated through comparisons with foreign products and testing roads, complemented by rapid dissolution tests to determine Iceguard's service life [25,26].

Through research and the application of ice-suppressing materials both in China and abroad, it becomes evident that current ice-suppressing material technologies are in their initial and exploratory stages. A comprehensive set of technical evaluation indicators and quality control standards for ice-suppressing materials has yet to be established, and ongoing project applications remain in the testing phase [27,28].

The ice-suppressing material developed in this study exhibits several key characteristics: active deicing, no adverse impact on roads, bridges, ancillary facilities, and vegetation, preventive pavement maintenance, and continuous winter deicing. This presents a novel approach to road deicing. The composition design method for the ice-suppressing material is proposed, and considering the material's unique characteristics, a performance evaluation methodology is introduced. This evaluation serves as a theoretical foundation for the widespread adoption of asphalt pavement ice-suppressing materials.

2. Materials and Methods

2.1. Deicing Performance Test Methods of Ice-Suppressing Materials

One crucial functional aspect of ice-suppressing materials is their deicing effectiveness. Anti-freezing/anti-icing tests, hydrophobic property assessments, adhesion property examinations, and ice-melting property tests are employed to assess the deicing performance of these materials.

2.1.1. Anti-Icing Test Method

This paper utilizes the kinetic energy generated by the free fall of a steel ball to simulate the force required for ice removal from the road surface equivalently. The magnitude of the adhesion force between the ice and the road surface is determined by the cracking of the ice layer, as illustrated in Figure 1, depicting the test principle.

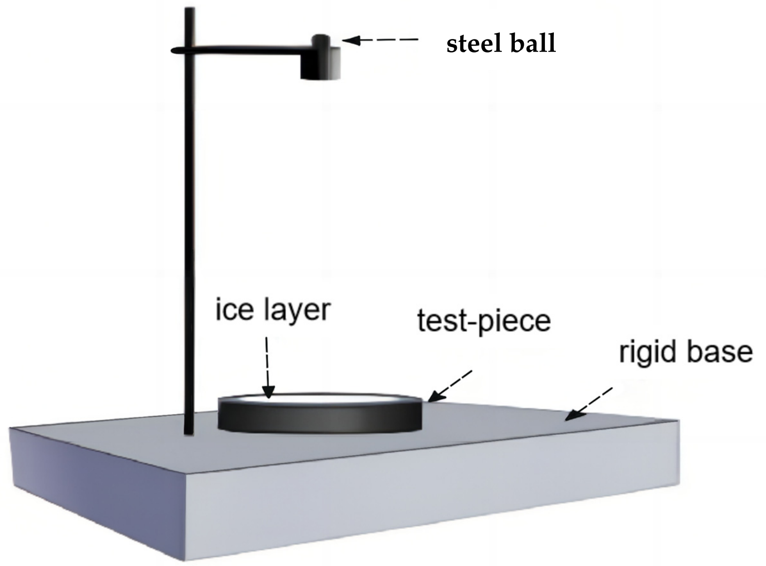

Figure 1. Principle diagram of falling ball impact test.

A qualitative method was used to observe the cracking and breaking condition of the ice surface to evaluate the anti-icing effect as shown in Table 1.

Table 1. Anti-icing effect evaluation method.

Anti-Icing Effect	Ice Surface Condition
Excellent	Significant breakage and peeling on the ice surface
Good	Small amount of breakage and cracks on the ice surface
Medium	Only a few cracks on the ice surface
Bad	The only marks on the ice surface are from the impact of the steel ball

To enhance the precision of assessing the anti-icing effect of the ice-suppressing material, the breakage rate index is introduced by drawing on the pavement structure layer damage evaluation index. The calculation formula for the breakage rate is depicted in Equation (1) [29].

$$B_R = \frac{B_A + \lambda L}{A} \tag{1}$$

where

B_R—breakage rate, expressed in percentage, %.
B_A—Total area of crushing and cracking, cm^2.
L—extended single crack length, cm.
λ—Influence factor for converting single cracks to area, generally taken as 0.3.
A—Total area of the test, cm^2.

2.1.2. Hydrophobic Performance Test Method

The hydrophobic performance of ice-suppressing materials plays a crucial role in the deicing effectiveness of asphalt pavement. Therefore, evaluating the hydrophobic performance after application is essential. Hydrophobic performance is typically assessed by measuring the contact angle (θ). It is generally considered that when $\theta > 90°$, the material is hydrophobic, while $\theta < 90°$ indicates hydrophilic properties. A larger contact angle (θ) signifies superior hydrophobic performance. Currently, methods for measuring the contact angle include angle measurement, height measurement, force measurement, droplet image analysis, and transmission methods, among others [29].

With advancements in image processing technology, the droplet image analysis method offers higher accuracy and simplifies the measurement process. In this study, the contact angle is calculated using the droplet image analysis fitting method [30]. The following steps are involved:

Droplet edge acquisition methods can be categorized into automatic image processing and manual image processing. Each method has its own advantages and disadvantages. Automatic image processing offers fast acquisition but requires further research to enhance its resistance to interference. Manual processing, on the other hand, exhibits strong interference resistance but involves a significant workload. The contact angle can be calculated using methods such as the tangent method, circle fitting method, ellipse fitting method, Young–Laplace method, and polynomial fitting method.

Based on the aforementioned theory and methodology, the contact angle is determined by creating ice-suppressing material samples. A high-resolution digital camera is used to capture droplet morphology, and Image-Pro Plus or CAD image processing software (version 2.8) is employed for analysis. The specific steps are outlined as follows:

Preparation of ice-suppressing material samples.

Application of the prepared material sample onto glass slides or microscope slides, followed by curing at room temperature.

Spraying droplets onto the surface of the glass slides coated with the cured deicing material.

Recording and photographing the process of droplet morphology change using a high-resolution digital camera positioned perpendicular to the slide's plane.

The contact angle is then plotted and calculated using image processing software.

2.1.3. Adhesion Performance Test Method

The force per unit area required to bond the bonding material is referred to as bond strength. Common methods for measuring bond strength include the three-point bending test, shear strength test, and tensile strength test. The primary purpose of the tensile and shear tests is to quantitatively assess the adhesion between the ice-suppressing material sprayed on the specimens and the ice cubes. To clearly reveal the deicing capability of the coated ice-suppressing material test specimens, comparative tests were conducted between the spraying group and the control group.

Two cylindrical specimens of asphalt mixture were prepared, securely fixed, and filled with water in the middle. Subsequently, they were placed in a freezer and frozen under conditions simulating real-world scenarios. The test temperature was set at −30 °C, and the freezing duration was 12 h. Afterward, the test specimens were removed from the freezer, and both tensile and shear tests were immediately conducted using a 100 KN universal testing machine. The principles of the tensile and shear tests are illustrated in Figures 2 and 3, respectively.

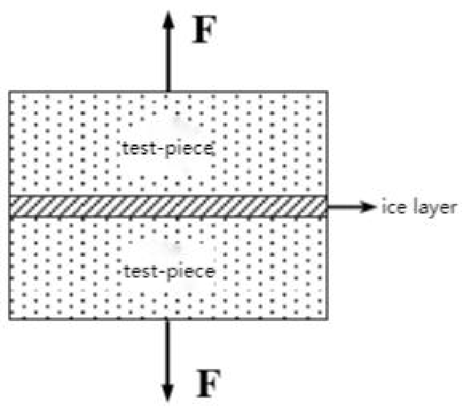

Figure 2. Tensile test schematic.

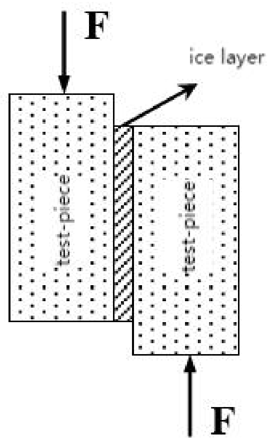

Figure 3. Shear test schematic.

2.2. Design of the Composition of the Ice-Suppressing Material

To enhance the deicing capabilities of the pavement without compromising its skid resistance, a systematic experimental study was undertaken to formulate an ice-suppressing material characterized by long-lasting- and slow-release properties. The ultimate composition of the ice-suppressing material comprises three key components: film-forming component A, adhesive component B, and ice suppression component C.

2.2.1. Modified Ice Suppression Component C Composition Design

In accordance with the design of the ice suppression function within the ice-suppressing material, component C should incorporate the freezing point inhibitor C1, which necessitates a porous adsorption carrier C2 for adsorption. Therefore, the ice-suppressing material includes the porous adsorption carrier C2. To prevent the ice-suppressing material from altering the road surface's color, a small amount of carbon black component C3 is added to enhance the color of the ice-suppressing material powder. The ice suppression component powder is adjusted using a modified coupling agent C4 to enhance its dispersibility [31].

The adsorption capacity of the porous adsorption carrier material C2 for the freezing point inhibitor C1 can be quantitatively expressed by the mass change before and after adsorption, referred to as the adsorption rate. The specific test procedure is as follows: weigh the porous adsorption carrier material C2 with a mass of m_0 (accurate to 0.01 g) after drying. Subsequently, immerse it in a pre-prepared saturated solution of the ice point inhibitor C1 and remove it after 24 h. Weigh the mass m1 after drying in a low-temperature drying oven at 110 °C, and calculate the adsorption rate of the porous adsorption carrier material using the Formula (2).

$$S_a = \frac{m_1 - m_0}{m_0} \tag{2}$$

where

m_1 is the mass of the material after immersion.
m_0 is the mass of the material before immersion.
S_a is the adsorption rate of the porous adsorption carrier material.

The optimal ratio of freezing point inhibitor C1 to porous adsorption carrier C2 can be determined using the adsorption rate test method described above. The test results are presented in Table 2.

Table 2. Adsorption performance test results.

Time (h)	Mass of the Material before Immersion m_0 (g)	Mass of the Material after Immersion m_1 (g)	Adsorption Rate (%)
2	100	122.21	22.21
4	100	134.31	34.31
6	100	144.33	44.33
8	100	149.42	49.42
10	100	152.17	52.17
12	100	153.32	53.32
14	100	154.02	54.02
16	100	154.33	54.33
18	100	154.45	54.45
20	100	154.45	54.45
22	100	154.45	54.45
24	100	154.45	54.45

It can be observed from Table 2 that the adsorption rate of the porous adsorption carrier increases over time, and the rate of increase becomes gradual. After 18 h, the adsorption rate of the porous adsorption carrier material reaches a plateau and stabilizes, indicating that the porous adsorption carrier has reached saturation. Consequently, it can be concluded that the mass ratio of the porous adsorption carrier C2 to the freezing point inhibitor C1 is C2:C1 = 100:54. The proportions of carbon black C3 and modified silane coupling agent C4 in the composite freezing point inhibitor C1 and porous adsorption carrier C2 can be determined based on practical experience and adsorption performance tests, as presented in Table 3.

Table 3. Modified ice suppression component C composition ratio.

Ingredients	Proportion of Each Component (%)
Complex freezing point inhibitor C1	54
Porous adsorption carrier C2	100
Carbon black C3	2.5
Modified silane coupling agent C4	1.6

2.2.2. Composition Design of Film-Forming Component A

In accordance with the hydrophobic function design of the ice-suppressing material, the composition of the film-forming component A should include the hydrophobic road bonding material, silicone-rubber lotion A1, along with various additives and fillers. These include a reinforcing agent A2, filler A3, film-forming agent A4, plasticizer A5, catalyst A6, leveling agent A7, defoamer A8, diluent water A9, and anti-skid material quartz sand A10. The additives serve to promote the plastic flow and elastic deformation of silicone rubber lotion, enhancing its bonding performance and facilitating effective film-forming. Fillers play a role in reinforcing silicone rubber and improving its tensile strength.

The ratio of silicone rubber lotion A1 to diluent water was analyzed through hydrophobic and adhesive tests. Multiple portions of organic silicone rubber lotion with a mass of 100 g and a solid content ranging from 20% to 60% were weighed. The organic silicone rubber lotion was then mixed with diluent water A9 in proportions ranging from 20 g to 300 g, respectively. Subsequently, hydrophobic property tests and adhesion property tests were conducted. The contact angle was measured using the height method, while tensile and shear forces were measured using a UTM machine. The results of these tests are presented in Table 4.

Table 4. Hydrophobic and adhesion test results.

Silicone Rubber Emulsion (g)	Diluent (g)	Contact Angle (°)	Hydrophobic Grade	Tensile Force (N)	Shear Force (N)
100	20	90.2	HC1	1644	10,506
100	60	96.3	HC1	1478	8056
100	100	102	HC1	1354	6537
100	140	108.5	HC1	1259	5245
100	180	112.1	HC1	1215	4165
100	220	109.3	HC1	1242	5148
100	260	107.4	HC1	1340	6449
100	300	98.2	HC1	1537	8730

According to the results of the hydrophobic and adhesion tests presented in Table 4, it is observed that the contact angle in the hydrophobic test initially increases and then decreases with an increase in the quality of the diluent. Conversely, the tensile force and shear force in the adhesion test exhibit a decreasing trend followed by an increase as the quality of the diluent increases. These trends suggest that as the quality of the diluent gradually increases, the hydrophobicity of the ice-suppressing material first increases and then decreases, while the adhesion property decreases initially and then increases. The optimal performance is achieved when the contact angle is at its maximum, and the tensile force and shear force are at their minimum, which occurs when the mass of the diluent is 180 g. At this point, the ice-suppressing material exhibits the best anti-icing performance. Simultaneously, the ideal ratio of silicone rubber lotion A1 to diluent A9 is A1:A9 = 100:180. Based on practical experience, hydrophobic property tests, and adhesive property tests, as summarized in Table 5, it is possible to determine the optimal ratio of each component in the film-forming component.

Table 5. Composition ratio of film-forming component A.

Ingredients	Proportion of Each Component (%)
Silicone rubber emulsion A1 with a solid content of 20%~60%	100.0
Reinforcing agent A2	4.0
Packing A3	3.0
Film-forming agent A4	4.0
Plasticizer A5	4.2
Catalyst A6	1.7
Levelling agent A7	3.0
Defoamer A8	0.3
Diluent A9	180.0
Anti-slip quartz sand A10	3.0

2.2.3. Adhesive Component B Composition Design

The role of the adhesive component is to accelerate the reaction speed between the components of the ice-suppressing material and speed up the time of opening traffic. The adhesive component is composed of cross-linking agent B1 and coupling agent B2. Based on actual experience, the proportion of the components of the cross-linking agent and coupling agent is usually taken as shown in Table 6.

Table 6. Composition ratio of gluing component B.

Ingredients	Proportion of Each Component (%)
Cross-linking agent B1	29
Coupling agent B2	71

2.2.4. Ice-Suppressing Material A, B, C Composition Ratio

(1) Determination of the mass ratio of component B

Prepare components A and C according to the optimum composition of each component determined in advance for components A and C. The preparation principle involves dispersing component C evenly into component A to prevent agglomeration. The A:C mass ratio is 100:2. Component C should be slowly poured into component A to create the mixture of components A and C according to this specified ratio. Then, various quantities of component B are added to the previously prepared mixture of components A and C to create the ice-suppressing material. Under conditions where the spraying temperature is 5 °C, and the spraying rate of the ice-suppressing material is 0.5 kg/m^2, Marshall test specimens are fabricated according to the anti-icing test method.

The three components of the ice-suppressing material will undergo a curing reaction after mixing. The curing time of the ice-suppressing material includes two phases: the curing time in the spraying equipment and the interval of time from when the ice-suppressing material is sprayed on the road to when it completely solidifies. The curing time of the ice-suppressing material in the spraying equipment is referred to as the pre-curing time, while the time from when the ice-suppressing material is sprayed onto the road surface until it completely solidifies is termed the post-curing time. The post-curing time of the Marshall test specimens was measured, and the "falling ball impact test" was conducted. The test results are presented in Table 7.

Table 7. Falling ball impact test results.

(A + C) Component Mass (g)	Mass of Component B (g)	Post-Curing Time (h)	Breakage Rate (%)
100	0.5	7.2	17.9
100	1.0	5.3	17.8
100	1.5	3.8	17.7
100	2.0	3.1	17.6
100	2.5	2.5	15.5
100	3.0	1.7	12.4
100	3.5	0.6	9.9
100	4.0	0.2	6.2

Table 7 reveals that the post-curing time of the test specimen gradually decreases with an increase in the mass of component B, and the damage rate of the test specimen decreases as well. When component B is less than 2 g, the damage rate decreases slowly, but when component B exceeds 2 g, the damage rate decreases significantly. This suggests that when component B exceeds 2 g, the deicing performance is noticeably reduced. Taking into account both the deicing performance of the ice-suppressing material and its impact on traffic due to post-curing time, the mass of component B should be 2 g, and the mass ratio of (A + C):B should be 100:2.

(2) Determination of the mass ratio of component A and C

Under the condition of a mass ratio of (A + C):B = 100:2, different proportions of components A and C were used to formulate the ice-suppressing material. The results of the "falling ball impact test" and bonding performance test, conducted in accordance with the anti-icing test method, are presented in Table 8. From the results in Table 8, it is evident that as the mass of component C gradually increases, the breakage rate also increases progressively. The rate of increase levels off when component C exceeds 3 g. Additionally, the tensile force and bonding force gradually decrease with an increase in the mass of component C, and the rate of reduction levels off as well. Therefore, it is recommended that the mass ratio of component A and C be set at 97:3 to fully address the deicing performance of the ice-suppressing material.

Table 8. Falling ball impact test and bonding performance test.

Mass of Component A (g)	Mass of Component C (g)	Mass of Component B (g)	Breakage Rate (%)	Tensile Force (N)	Shear Force (N)
99.5	0.5	2.0	5.8	1753	10,513
99.0	1.0	2.0	9.8	1629	9238
98.5	1.5	2.0	12.9	1537	8295
98.0	2.0	2.0	15.4	1454	7450
97.5	2.5	2.0	17.4	1379	6697
97.0	3.0	2.0	18.2	1304	6148
96.5	3.5	2.0	18.4	1237	5685
96.0	4.0	2.0	18.6	1181	5282
95.5	4.5	2.0	18.7	1151	4906
95.0	5.0	2.0	18.7	1129	4549
94.5	5.5	2.0	18.7	1110	4275
94.0	6.0	2.0	18.7	1095	4034

In summary, the mass ratio of components A, B, and C is determined as follows: $m_A:m_B:m_C$ = 97:2:3.

3. Results and Discussion

3.1. Analysis of Anti-Icing Test Results

Two sets of Marshall specimens and rutting plate specimens were prepared using AC-13 grade asphalt mixture with an asphalt-aggregate ratio of 5.0%. One set of Marshall specimens and rutting plate specimens were subjected to a spraying treatment with an ice-suppressing material at a rate of 0.5 kg/m^2, while the other set of Marshall specimens and rutting plate specimens were left untreated. The testing procedures followed the anti-icing test protocol, including the falling ball impact test. Figures 4 and 5 illustrate the Marshall specimens after the falling ball impact test and the gravity knockdown test, respectively. Figure 6 depicts the rutting plate specimens following the falling ball test.

Unsprayed Sprayed

Figure 4. Marshall specimens after falling ball impact test.

Sprayed group specimen Unsprayed group specimen

Figure 5. Marshall specimens after gravity knockdown test.

Without spraying group specimen Sprayed group specimen

Figure 6. Rutting plate specimens after falling ball impact.

From Figure 4, it can be deduced that the surface of the Marshall specimen in the contrast group (left) displays only steel ball impact marks and pits. In contrast, the surface of the Marshall specimen in the spraying group (right) exhibits clear fracture boundaries, and there is no residual ice adhesion in the fractured areas. This qualitative assessment suggests that the ice-suppressing substance has a superior anti-icing effect. The calculated ice broken area is 12.72 cm^2, determined through indoor measurements of the Marshall specimen in the spraying group, resulting in a calculated breakage rate of 16.2%.

Figure 5 demonstrates that the ice layer on the surface of the sprayed Marshall specimen can be completely removed by gravity, leaving no residual dark ice on the specimen's surface. Conversely, the Marshall specimen in the contrast group (unsprayed) exhibits substantial dark ice, indicating a higher adhesion between the ice layer and the specimen in the contrast group compared to the spraying group.

Regarding the falling ball impact test of the rutting plate specimen shown in Figure 6, it can be inferred that the ice layer on the rutting plate specimen in the contrast group partially detaches in a small area after impact, with most of the ice layer remaining attached to the specimen. In contrast, the rutting plate specimen sprayed with the ice-suppressing material experiences a significant detachment of the ice layer over a large area, with no dark ice remaining on the rutting plate after the fall. This suggests that the ice-suppressing material effectively isolates the ice layer from the specimen, and the ice layer on the specimen treated with the ice-suppressing material is easily removed.

3.2. Analysis of Hydrophobic Performance Test Results

In accordance with the test procedure of the droplet image analysis method, water droplets were placed on the surfaces of both uncoated glass slides and glass slides coated with the ice-suppressing material. Photographs were taken at various time intervals (5 s, 30 s, 2 min, 4 min, 6 min, 8 min, 10 min, 12 min, 14 min, 16 min, 18 min, 20 min). The comparison of static contact angles from the test results is presented in Figure 7. In each image, the droplets on the left side are on regular glass slides (contrast group), and those on the right side are on slides coated with the ice-suppressing material (spraying group). The change in droplet contact angles over time is illustrated in Figure 8.

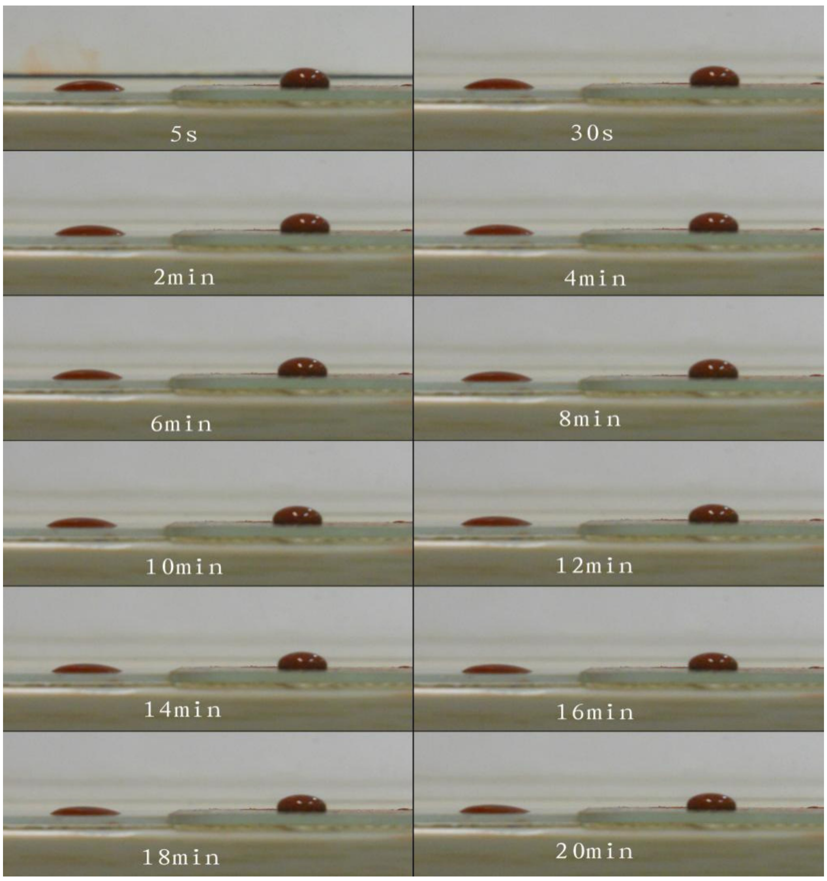

Figure 7. Real-time image of liquid drop contact angle.

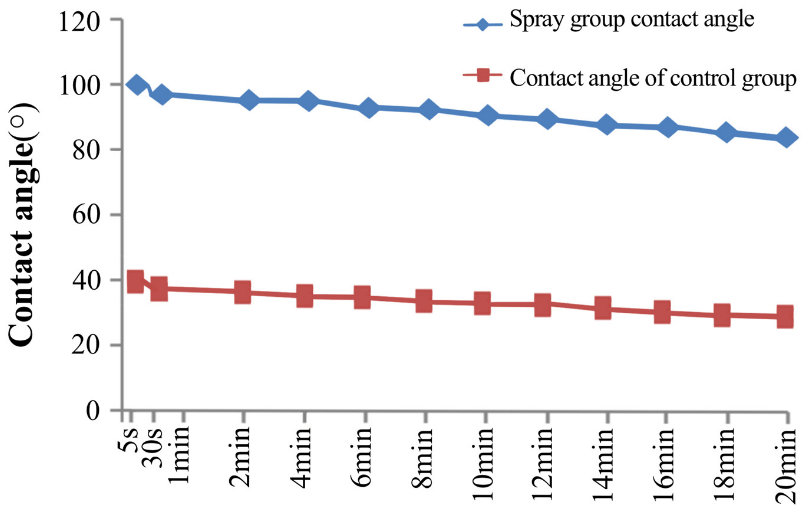

Figure 8. Plot of droplet contact angle over time.

Figure 8 demonstrates the temporal evolution of droplet contact angles. The contact angle gradually decreases as time progresses, primarily due to water droplet evaporation and the gradual spreading of droplets on the slide's surface. To minimize errors and obtain more accurate contact angle measurements, it is advisable to measure the contact angle as quickly as possible.

For droplets on slides coated with the ice-suppressing material, the contact angle was 99.5° at 5 s and gradually decreased to 83.3° at 20 min. In contrast, the contact angle for droplets on clean slides ranged from 39.2° to 29° over the same time period. A comparison of the data leads to the conclusion that the ice-suppressing material exhibits excellent hydrophobic properties and significantly reduces the adhesion between the ice layer and the road surface.

3.3. Analysis of Adhesion Performance Test Results

In accordance with the test methods and procedures for assessing adhesion performance, asphalt mixture specimens that were sprayed with ice-suppressing material and contrast asphalt mixture specimens that remained unsprayed were subjected to both tensile and shear tests. The interfaces between the ice layer and the specimens after the tensile and shear tests are visually depicted in Figures 9 and 10, while the results of these tests are presented in Figure 11.

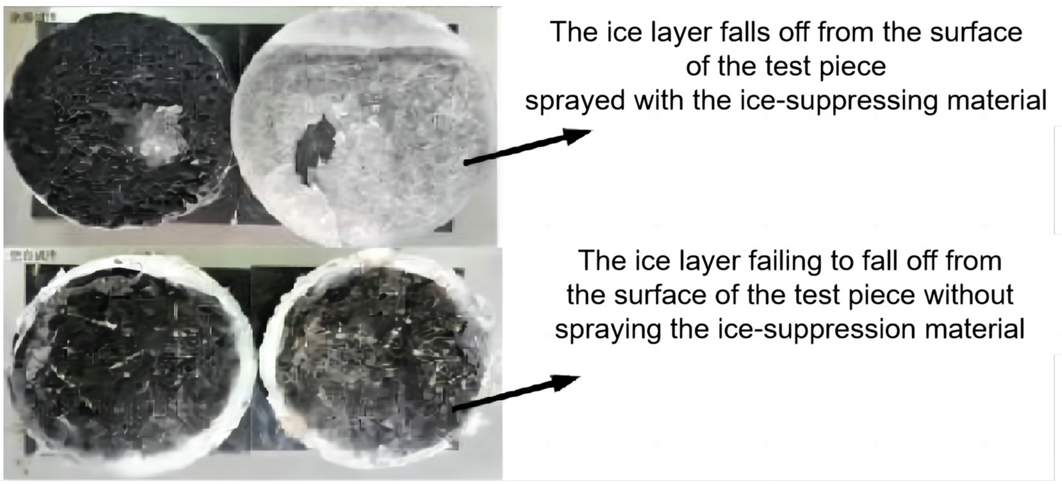

Figure 9. Ice–sample interface after tensile test damage.

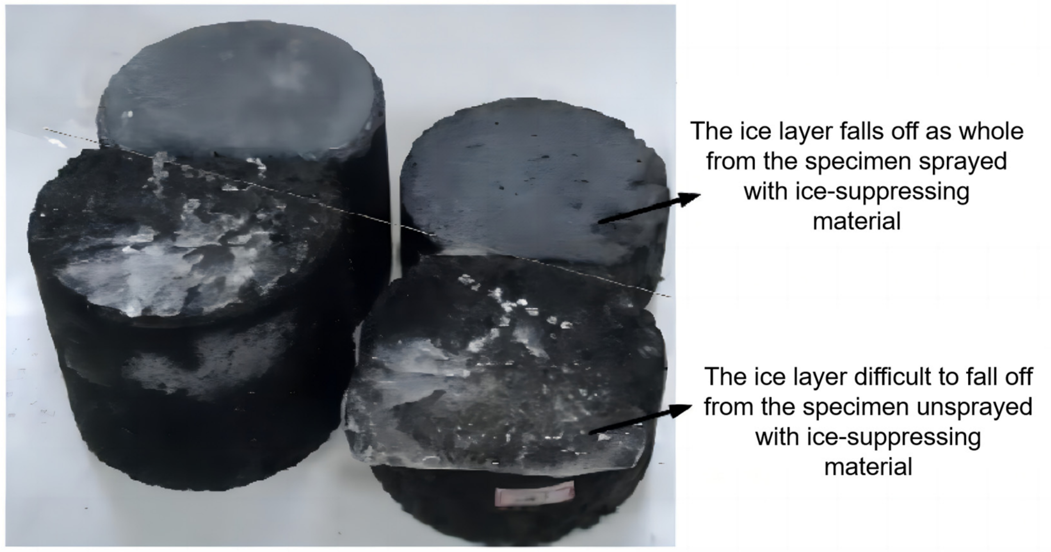

Figure 10. Ice–sample interface after shear test damage.

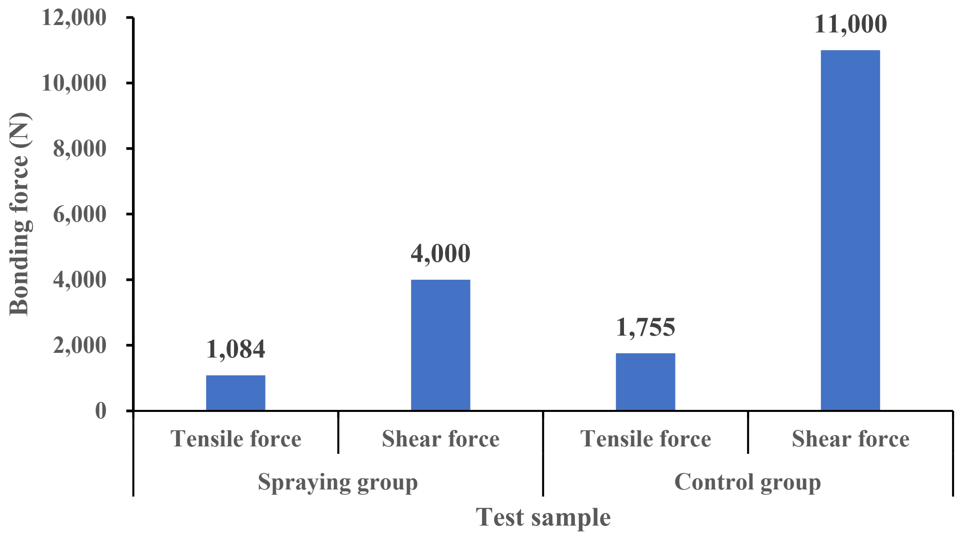

Figure 11. Test results of adhesion performance of specimens in spraying group and unsprayed contrast group.

The tensile test results presented in Figure 11 indicate that, in the case of the sprayed group specimen, the ice layer becomes detached from the specimen when the tensile force reaches 1084 N. Additionally, there is virtually no dark ice remaining on the specimen's surface, and the cross-section appears flat. This phenomenon is attributed to the chemical action of the freezing point inhibitor, which results in the interface's strength becoming weaker than that of the ice, leading to fracture at the interface.

In contrast, for the unsprayed contrast group specimen, the ice layer becomes detached from the specimen when the tensile force reaches 1755 N. In this case, the two specimens break from the middle of the ice layer, leaving a substantial amount of dark ice on the specimen's surface. The cross-section between the test piece and the ice layer exhibits a conical shape. The tensile force between the ice layer and the surface of the test piece, after being treated with the ice-suppressing material, is reduced by 38.2% compared to the untreated specimen. This lower tensile force indicates a weaker adhesive force between the ice-suppressing material test piece and the ice layer, making it easier to remove the ice layer.

The shear test results reveal that, when subjected to shear force, the sprayed group specimens detach from the ice layer when the shear force reaches 4000 N. Similar to the tensile test, there is minimal dark ice remaining on the specimen's surface, and the cross-section appears flat. In contrast, the unsprayed contrast group specimens detach from the ice layer under shear force reaching 11,000 N. In this case, the two specimens break from the middle of the ice layer, leaving a substantial amount of dark ice on the specimen's surface. The cross-section between the test piece and the ice layer exhibits a conical shape, similar to the results of the tensile test. After applying the ice-suppressing material, the shear force between the ice layer and the specimen's surface is reduced by 63.6%. A lower shear force is advantageous for crushing the ice layer under the wheel's pressure.

3.4. Ice-Melting Performance Test and Result Analysis

The effectiveness of the ice-suppressing material in melting ice is a crucial factor that influences the separation of the ice layer from the asphalt pavement. The ice-suppressing material works by melting the lower surface of the ice layer, leading to the separation of the ice layer from the asphalt pavement. To simulate the ice-melting performance of the ice-suppressing material on the ice layer, the following test method and procedure were employed.

Marshall test specimens were prepared for both the spraying group and the unsprayed contrast group. Each group had a total ice mass of 60 g, and the test was conducted at −30 °C, with the temperature increasing by 2 °C every hour. To minimize the temperature-induced changes in ice mass, the maximum temperature was limited to 0 °C. The results of the ice-melting performance test are presented in Table 9 and Figure 12.

Table 9. Ice-melting performance test results.

Temperature (°C)	Sprayed Group Ice Mass (g)	Unsprayed Group Ice Mass (g)
−30	60	60
−25	57	59
−20	51	57
−15	43	52
−10	32	45
−5	19	35
0	4	23

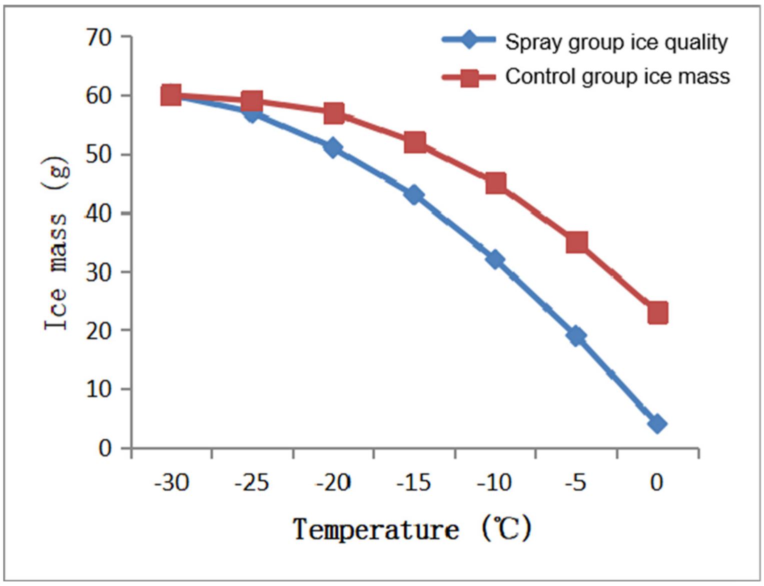

Figure 12. Ice-melting performance test results graph.

Figure 12 illustrates the relationship between temperature and the mass reduction in ice cubes. As the temperature increases, the mass of the ice cubes gradually decreases, and the rate of mass reduction steadily increases. Notably, at the same temperature, the mass reduction rate of the unsprayed group's ice cubes is significantly lower than that of the sprayed group's ice cubes. This observation, after accounting for the influence of temperature rise on the change in ice cube mass, suggests that the ice-suppressing material exhibits excellent ice-melting performance.

4. Conclusions

In consideration of the characteristics of the ice-suppressing material, a test method for evaluating its deicing performance was proposed, focusing on key technologies related to the material and the selection principles for its key component materials. Through the evaluation of the deicing performance method, the composition proportions of each component in the ice-suppressing material were determined. A comprehensive study and analysis of its performance was conducted, with a particular focus on its deicing capabilities and durability. The primary conclusions drawn from this research are as follows:

(1) In consideration of the characteristics of the ice-suppressing material, an evaluation method for assessing its deicing performance was proposed. The material's hydrophobicity was assessed by measuring the contact angle using the droplet image analysis method. Tensile and shear tests were employed to evaluate the material's adhesion to the ice layer.

(2) According to the characteristics of the ice-suppressing material, the proposed evaluation method for the deicing performance is used to design the components of the ice-suppressing material. Through analysis, the mass ratio of component A, component B, and component C is m_A:m_B:m_C = 97:2:3.

(3) The ice-suppressing material demonstrates an effective isolation effect between the ice layer and the test specimen, leading to easy detachment of the ice layer from the test specimen when the material is applied.

(4) The contact angle of water droplets on glass slides coated with the ice-suppressing material (θ) exhibits a variation ranging from 99.5° to 83.3°, while the contact angle of water droplets on clean glass slides ranges from 39.2° to 29°. A larger contact angle indicates stronger hydrophobicity, thereby signifying enhanced hydrophobic properties of the ice-suppressing material.

(5) The tensile strength of the ice layer and the coated ice-suppressing material specimen has decreased by 38.2%, and the shear strength has reduced by 63.6% compared to the uncoated ice-suppressing material specimen. This reduction suggests that the ice-suppressing material effectively diminishes the adhesion between the ice layer and the specimen, facilitating easier detachment of the ice layer.

(6) Under external conditions with temperatures below 0 °C, the mass reduction rate of ice cubes in the uncoated group is significantly lower than that of ice cubes in the coated group. After accounting for the influence of temperature on the change in ice cube mass, this observation confirms the excellent ice-melting performance of the ice-suppressing material.

Author Contributions: Conceptualization, Y.Z.; methodology, Y.Z.; software, Y.Z.; validation, M.Z.; formal analysis, M.Z.; investigation, X.Z.; resources, M.Z.; data curation, X.Z.; writing—original draft preparation, X.Z.; writing—review and editing, X.Z.; visualization, X.Z.; supervision, X.Z.; project administration, M.Z.; funding acquisition, M.Z. All authors have read and agreed to the published version of the manuscript.

Funding: This research was funded by and the project was supported by the introduction of talents and scientific research start-up Fund of Nanjing Institute of Technology, grant number No. YKJ201834 and the project was supported by the Open Research Fund of NJIT Institute of Industrial Economy and Innovation Management (No. JGKA202204).

Institutional Review Board Statement: Not applicable.

Informed Consent Statement: Not applicable.

Data Availability Statement: No new data was created.

Conflicts of Interest: The authors declare no conflicts of interest.

References

1. Shen, F.; Wei, G.; Pang, R.; Liu, F.; Fang, S. Performance Evaluation of a Hydrophobically Modified Anti-Slide and Anti-icing Coating. *IOP Conf. Ser. Mater. Sci. Eng.* **2019**, *688*, 033004. [CrossRef]
2. Wang, T.; Dra, Y.A.S.S.; Cai, X.; Cheng, Z.; Zhang, D.; Lin, Y.; Yu, H. Advanced cold patching materials (CPMs) for asphalt pavement pothole rehabilitation: State of the art. *J. Clean. Prod.* **2022**, *366*, 133001. [CrossRef]
3. Pytka, J. Determination of snow stresses under vehicle loads. *Cold Reg. Sci. Technol.* **2010**, *60*, 137–145. [CrossRef]
4. Xu, S.; Zhou, Z.; Feng, L.; Cui, N.; Xie, N. Durability of pavement materials with exposure to various anti-icing strategies. *Processes* **2021**, *9*, 291. [CrossRef]
5. Ma, T.; Geng, L.; Ding, X.; Zhang, D.; Huang, X. Experimental study of deicing asphalt mixture with anti-icing additives. *Constr. Build. Mater.* **2016**, *127*, 653–662. [CrossRef]
6. Huang, K.; Liu, J.; Wang, J.; Shi, X. Characterization and Mechanism of a New Superhydrophobic Deicing Coating Used for Road Pavement. *Crystals* **2021**, *11*, 1304. [CrossRef]
7. Pei, Z.; Yi, J.; Li, Y.; Cheng, P.; Zhu, Y.; Feng, D. Material design and performance analysis of the anti-ice and antiskid wear layer on pavement. *Constr. Build. Mater.* **2021**, *282*, 122734. [CrossRef]
8. Yang, M. Research on Application Technology of Self Melting Ice Fine Surface Treatment. In *Hydraulic and Civil Engineering Technology VI: Proceedings of the 6th International Technical Conference on Frontiers of HCET 2021*; IOS Press: Amsterdam, The Netherlands, 2021; p. 348.
9. Jiang, X.; Gabrielson, J.; Titi, H.; Huang, B.; Bai, Y.; Polaczyk, P.; Hu, W.; Zhang, M.; Xiao, R. Field investigation and numerical analysis of an inverted pavement system in Tennessee, USA. *Transp. Geotech.* **2022**, *35*, 100759. [CrossRef]
10. Ma, R.; Sun, H.; Tian, Z. Study on preparation and performance of slow-release pavement snow melting salt. In *Frontier Research: Road and Traffic Engineering*; CRC Press: Boca Raton, FL, USA, 2022; pp. 383–388.
11. Yang, Y.; Chen, G.; Yang, Y.; Yue, L.; Xu, J. Advances in Salt-Storage Materials, Road and Anti-Freezing Performances of Salt-Storage Asphalt Mixture: A Review. *Coatings* **2022**, *12*, 1323. [CrossRef]
12. Wang, T.; Wei, X.; Zhang, D.; Shi, H.; Cheng, Z. Evaluation for Low Temperature Performance of SBS Modified Asphalt by Dynamic Shear Rheometer Method. *Buildings* **2021**, *11*, 408. [CrossRef]
13. Yu, W.; Yi, X.; Guo, M.; Chen, L. State of the art and practice of pavement anti-icing and de-icing techniques. *Sci. Cold Arid Reg.* **2014**, *6*, 14–21.
14. Yu, H.; He, Z.; Qian, G.; Gong, X.; Qu, X. Research on the anti-icing properties of silicone modified polyurea coatings (SMPC) for asphalt pavement. *Constr. Build. Mater.* **2020**, *242*, 117793. [CrossRef]
15. Chen, Y.; Tan, Y.; She, H.; Zhang, M.; Jiang, X.; Guo, P.; Li, Y.; Zhang, Y. Characteristics of slow-release ice and snow melting micro-surfacing materials. *Int. J. Pavement Eng.* **2022**, *24*, 2120986. [CrossRef]
16. Zhong, K.; Sun, M.; Chang, R. Performance evaluation of high-elastic/salt-storage asphalt mixture modified with Mafilon and rubber particles. *Constr. Build. Mater.* **2018**, *193*, 153–161. [CrossRef]
17. Zheng, M.; Zhou, J.; Wu, S.; Yuan, H.; Meng, J. Evaluation of long-term performance of anti-icing asphalt pavement. *Constr. Build. Mater.* **2015**, *84*, 277–283. [CrossRef]
18. Jiang, X.; Zhu, H.; Yan, Z.; Zhang, F.; Ye, F.; Li, P.; Zhang, X.; Dai, Z.; Bai, Y.; Huang, B. A state-of-art review on development and progress of backfill grouting materials for shield tunneling. *Dev. Built Environ.* **2023**, *16*, 100250. [CrossRef]
19. Chen, J.; Ma, X.; Wang, H.; Xie, P.; Huang, W. Experimental study on anti-icing and deicing performance of polyurethane concrete as road surface layer. *Constr. Build. Mater.* **2018**, *161*, 598–605. [CrossRef]
20. Zhou, L.; Ding, L.; Yi, X. A review of snow melting and de-icing technologies for trains. *Proc. Inst. Mech. Eng. Part F J. Rail Rapid Transit* **2022**, *236*, 877–886. [CrossRef]
21. Shan, L.; Li, Z.; Tian, D.; Tan, Y. Effect of anti-icing additives on the stability of emulsified asphalt binders. *Constr. Build. Mater.* **2021**, *275*, 121951. [CrossRef]
22. Zhang, H.; Guo, R. Investigation of Long-Term Performance and Deicing Longevity Prediction of Self-Ice-Melting Asphalt Pavement. *Materials* **2022**, *15*, 6026. [CrossRef]
23. Zheng, M.; Wu, S.; Wang, C.; Li, Y.; Ma, Z.; Peng, L. A study on evaluation and application of snowmelt performance of anti-icing asphalt pavement. *Appl. Sci.* **2017**, *7*, 583. [CrossRef]
24. Peng, C.; Yu, J.Y.; Dai, J.; Zhao, Z.J.; Fu, J.Y.; Zhao, M.L.; Wang, W. Synthesis and property of a green melting-snow additive for asphalt pavement. *Appl. Mech. Mater.* **2014**, *694*, 85–89. [CrossRef]
25. Wang, T.; Weng, Y.; Cai, X.; Li, J.; Xiao, F.; Sun, G.; Zhang, F. Statistical modeling of low-temperature properties and FTIR spectra of crumb rubber modified asphalts considering SARA fractions. *J. Clean. Prod.* **2022**, *374*, 134016. [CrossRef]
26. Peng, C.; Yu, J.; Zhao, Z.; Dai, J.; Fu, J.; Zhao, M.; Wang, W. Synthesis and properties of a clean and sustainable deicing additive for asphalt mixture. *PLoS ONE* **2015**, *10*, e0115721. [CrossRef] [PubMed]

27. Wu, S.; Zheng, M.; Chen, W.; Bi, S.; Wang, C.; Li, Y. Salt-dissolved regularity of the self-ice-melting pavement under rainfall. *Constr. Build. Mater.* **2019**, *204*, 371–383. [CrossRef]
28. Wang, W.; Yu, J.Y.; Yi, Y.; Chen, X. Effect of De-Icing Additives on Aging Properties of Bitumen. *Mater. Sci. Forum* **2016**, *847*, 418–424. [CrossRef]
29. Wang, Z.; Zhang, T.; Shao, M.; Ai, T.; Zhao, P. Investigation on snow-melting performance of asphalt mixtures incorporating with salt-storage aggregates. *Constr. Build. Mater.* **2017**, *142*, 187–198. [CrossRef]
30. Akbari, R.; Antonini, C. Contact angle measurements: From existing methods to an open-source tool. *Adv. Colloid Interface Sci.* **2021**, *294*, 102470. [CrossRef]
31. Zhang, Y.; Zhao, X.; Zheng, M. Analysis of Engineering Performance and Environmental Impact of Asphalt Pavement Debonding and Ice Suppression Materials. *Buildings* **2023**, *13*, 689. [CrossRef]